Applications of the Lattice Boltzmann Method to Complex and Turbulent Flows

L.-S. Luo¹, D. Qi², and L.-P. Wang³

- ¹ ICASE, MS 132C, NASA Langley Research Center 3 West Reid Street, Building 1152, Hampton, Virginia 23681-2199, USA Email: luo@icase.edu; Homepapge: http://www.icase.edu/~luo
- Department of Paper and Printing Science and Engineering Western Michigan University, Kalamazoo, Michigan 49008, USA
- Department of Mechanical Engineering University of Delaware, Newark, Delaware 19716, USA

Abstract. We briefly review the method of the lattice Boltzmann equation (LBE). We show the three-dimensional LBE simulation results for a non-spherical particle in Couette flow and 16 particles in sedimentation in fluid. We compare the LBE simulation of the three-dimensional homogeneous isotropic turbulence flow in a periodic cubic box of the size 128³ with the pseudo-spectral simulation, and find that the two results agree well with each other but the LBE method is more dissipative than the pseudo-spectral method in small scales, as expected.

1 Introduction

More than a decade ago, the lattice-gas automata (LGA) [5,22,6] and the lattice Boltzmann equation (LBE) [16,12,2,20] were proposed as alternatives for computational fluid dynamics (CFD). Since their inception, the lattice-gas and lattice Boltzmann methods have attracted much interest in the physics community. However, it was only very recently that the LGA and LBE methods started to gain the attention from CFD community. The lattice-gas and lattice Boltzmann methods have been particularly successful in simulations of fluid flow applications involving complicated boundaries or/and complex fluids, such as turbulent external flow over complicated structures, the Rayleigh-Taylor instability between two fluids, multi-component fluids through porous media, viscoelastic fluids, free boundaries in flow systems, particulate suspensions in fluid, chemical reactive flows and combustions, magnetohydrodynamics, crystallization, and other complex systems (see recent reviews [3,15] and references therein).

Historically, models of the lattice Boltzmann equation evolved from the lattice-gas automata [5,22,6]. Recently, it has been shown that the LBE is a special discretized form of the continuous Boltzmann equation [8,9]. For the sake of simplicity without loss of generality, we shall demonstrate an *a priori* derivation of the lattice Boltzmann equation from the continuous Boltzmann equation with the single relaxation time (Bhatnagar-Gross-Krook) approximation [1]. The Boltzmann BGK equation can be written in the form of an

ordinary differential equation:

$$D_t f + \frac{1}{\lambda} f = \frac{1}{\lambda} f^{(0)}, \qquad f^{(0)} \equiv \frac{\rho}{(2\pi\theta)^{D/2}} \exp\left[-\frac{(\xi - u)^2}{2\theta}\right],$$
 (1)

where $D_t \equiv \partial_t + \boldsymbol{\xi} \boldsymbol{\nabla}, f \equiv f(\boldsymbol{x}, \boldsymbol{\xi}, t)$ is the single particle distribution function, λ is the relaxation time, and $f^{(0)}$ is the Boltzmann distribution function in D-dimensions, in which ρ , \boldsymbol{u} and $\theta = k_B T/m$ are the macroscopic density of mass, the velocity, and the normalized temperature, respectively, T, k_B and m are temperature, the Boltzmann constant, and particle mass. The macroscopic variables are the moments of the distribution function f with respect to the molecular velocity $\boldsymbol{\xi}$:

$$\rho = \int f \, d\boldsymbol{\xi} = \int f^{(0)} \, d\boldsymbol{\xi} \,, \tag{2a}$$

$$\rho \mathbf{u} = \int \boldsymbol{\xi} f \, d\boldsymbol{\xi} = \int \boldsymbol{\xi} f^{(0)} \, d\boldsymbol{\xi} \,, \tag{2b}$$

$$\rho\theta = \frac{1}{2} \int (\xi - u)^2 f \, d\xi = \frac{1}{2} \int (\xi - u)^2 f^{(0)} \, d\xi.$$
 (2c)

Equation (1) can be formally integrated over a time interval δ_t :

$$f(x + \xi \delta_t, \xi, t + \delta_t) = e^{-\delta_t/\lambda} f(x, \xi, t) + \frac{1}{\lambda} e^{-\delta_t/\lambda} \int_0^{\delta_t} e^{t'/\lambda} f^{(0)}(x + \xi t', \xi, t + t') dt'.$$
(3)

Assuming that δ_t is small enough and $f^{(0)}$ is smooth enough locally, and neglecting the terms of the order $O(\delta_t^2)$ or smaller in the Taylor expansion of the right hand side of (3), we obtain

$$f(x + \xi \delta_t, \xi, t + \delta_t) - f(x, \xi, t) = -\frac{1}{\tau} [f(x, \xi, t) - f^{(0)}(x, \xi, t)],$$
(4)

where $\tau \equiv \lambda/\delta_t$ is the dimensionless relaxation time. The equilibrium $f^{(0)}$ can be expanded as a Taylor series in \boldsymbol{u} up to \boldsymbol{u}^2

$$f^{(\text{eq})} = \frac{\rho}{(2\pi\theta)^{D/2}} \exp\left(-\frac{\boldsymbol{\xi}^2}{2\theta}\right) \left[1 + \frac{(\boldsymbol{\xi} \cdot \boldsymbol{u})}{\theta} + \frac{(\boldsymbol{\xi} \cdot \boldsymbol{u})^2}{2\theta^2} - \frac{\boldsymbol{u}^2}{2\theta}\right].$$
 (5)

To obtain the Navier-Stokes equations, the hydrodynamic moments $(\rho, \rho u, \text{ and } \rho \theta)$ and their fluxes must be preserved in finite discretized momentum space $\{\xi_{\alpha} | \alpha = 1, 2, \ldots, b\}$, *i.e.*,

$$\rho = \sum_{\alpha} f_{\alpha} = \sum_{\alpha} f_{\alpha}^{(\text{eq})}, \qquad (6a)$$

$$\rho \mathbf{u} = \sum_{\alpha} \boldsymbol{\xi}_{\alpha} f_{\alpha} = \sum_{\alpha} \boldsymbol{\xi}_{\alpha} f_{\alpha}^{(\text{eq})}, \qquad (6b)$$

$$\rho\theta = \frac{1}{2} \sum_{\alpha} (\boldsymbol{\xi}_{\alpha} - \boldsymbol{u})^2 f_{\alpha} = \frac{1}{2} \sum_{\alpha} (\boldsymbol{\xi}_{\alpha} - \boldsymbol{u})^2 f_{\alpha}^{(\text{eq})}, \qquad (6c)$$

where $f_{\alpha} \equiv f_{\alpha}(x, t) \equiv W_{\alpha} f(x, \xi_{\alpha}, t)$ [8,9]. It turns out that these moments can be evaluated *exactly* in discretized momentum space by using Gaussian-type quadrature [8,9,21].

We can derive the nine-velocity athermal LBE model on a square lattice in two-dimensions

$$f_{\alpha}(\boldsymbol{x}_{i} + \boldsymbol{e}_{\alpha}\delta_{t}, t + \delta_{t}) - f_{\alpha}(\boldsymbol{x}_{i}, t) = -\frac{1}{\tau}[f_{\alpha}(\boldsymbol{x}_{i}, t) - f_{\alpha}^{(\text{eq})}(\boldsymbol{x}_{i}, t)], \quad (7)$$

where the equilibrium $f_{\alpha}^{(\text{eq})}$, the discrete velocity set $\{e_{\alpha}\}$, and the weight coefficients $\{w_{\alpha}\}$ are given by

$$f_{\alpha}^{(\text{eq})} = w_{\alpha} \rho \left\{ 1 + \frac{3(e_{\alpha} \cdot u)}{c^2} + \frac{9(e_{\alpha} \cdot u)^2}{2c^4} - \frac{3u^2}{2c^2} \right\},$$
 (8a)

$$e_{\alpha} = \begin{cases} (0, 0), & \alpha = 0, \\ (\pm 1, 0)c, & (0, \pm 1)c, & \alpha = 1, 2, 3, 4, \\ (\pm 1, \pm 1)\sqrt{2}c, & \alpha = 5, 6, 7, 8, \end{cases}$$
(8b)

$$w_{\alpha} = \begin{cases} 4/9, & \alpha = 0, \\ 1/9, & \alpha = 1, 2, 3, 4, \\ 1/36, & \alpha = 5, 6, 7, 8, \end{cases}$$
 (8c)

and $c \equiv \delta_x/\delta_t$. Equation (7) involves only local calculations and uniform communications to the nearest neighbors. Therefore it is easy to implement and natural to massively parallel computers.

$$\rho \partial_t \boldsymbol{u} + \rho \boldsymbol{u} \cdot \nabla \boldsymbol{u} = -\nabla P + \rho \nu \nabla^2 \boldsymbol{u} \,, \tag{9}$$

with the isothermal ideal gas equation of state, the viscosity, and the sound speed given by

$$P = c_s^2 \rho$$
, $\nu = \left(\tau - \frac{1}{2}\right) c_s^2 \delta_t$, $c_s = \frac{1}{\sqrt{3}} c$. (10)

It should be noted that the factor -1/2 in the above formula for ν accounts for the numerical viscosity due to the second order derivatives of f_{α} . This correction in ν formally makes the LGA and LBE methods second order accurate. Similarly, we can derive the six-velocity and seven-velocity models on a triangular lattice in two-dimensions, and the twenty-seven-velocity models on a cubic lattice in three-dimensions [9].

There have been some significant progress made recently to improve the lattice Boltzmann method: (i) the generalized lattice Boltzmann equation with multiple relaxation times which overcomes some shortcomings of the lattice BGK equation [14]; (ii) use of grid refinement [4] and body-fitted mesh [10,7] with interpolation/extrapolation techniques; (iii) adaptation of unstructured grid by using the finite element method or the characteristic

Galerkin method; (iv) application of implicit scheme for steady state calculation and multi-grid technique to accelerate convergence (see a recent review [15] for further references).

In what follows we shall demonstrate the applications of the LBE method to simulate the flow of non-spherical particulate suspensions in fluid and homogeneous isotropic turbulence in a periodic box.

2 LBE Simulation of Flows of Non-Spherical Particulate Suspensions

The flow of particulate suspensions in fluid is difficult to quantify experimentally and to simulate numerically in some cases. Yet the flow of particulate suspensions is important to industrial applications such as fluidized beds. There have been some successful simulations of the flow of spherical suspensions by using conventional CFD methods, such as the finite element method. However, the simulation of the flow of non-spherical suspensions still remains as a challenge to the conventional CFD methods. Recently the LBE method has been successfully applied to simulate the flow of non-spherical suspensions in three-dimensions [17,18]. The success of the LBE method to this problem relies on the fact that the LBE method can easily handle the particle-fluid interfaces.

We first simulate a single non-spherical particle in the Couette flow. The equilibrium states in a non-spherical particulate suspension in a 3D Couette flow are simulated for a particle Reynolds number up to 320. Particle geometries include prolate and oblate spheroids, cylinders and discs. We show that the inertial effect at any finite Reynolds number qualitatively changes the rotational motion of the suspension, contrary to Jeffery's theory at zero Reynolds number [13]. At a non-zero Reynolds number, a non-spherical particle reaches an equilibrium state in which its longest and shortest axes are aligned perpendicular and parallel to the vorticity vector of the flow, respectively. This equilibrium state is unique, dynamically stable, fully determined by the inertial effect, the maximum energy dissipation state. Systems of either fifty cylinders or fifty discs in Couette flow are also simulated. Multi-particle interactions significantly change the equilibrium orientation of solid particle. The effect is stronger for cylinders than for discs. The details of this work will be reported elsewhere [19].

Figure 1 shows a 3D LBE simulation of sixteen cylindrical particles falling under the influence of gravity. The left figure illustrates the time evolution of the entire system of sixteen particles, while the right figure demonstrates the formation of inverted T configurations in the sedimentation, which has been observed experimentally. To the best of our knowledge, this phenomenon was first reproduced numerically by the LBE direct numerical simulation [18].

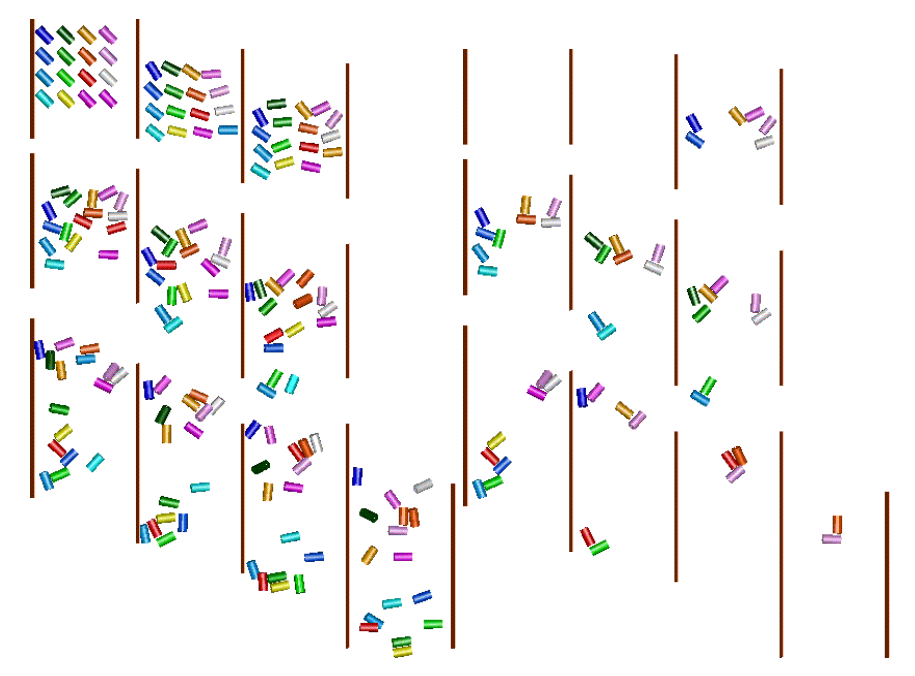


Fig. 1. 3D LBE simulation of particles sedimentation in fluid. Particle size is D=12 and L=24. System size is $N_x \times N_y \times N_z = 140 \times 150 \times 35$. The averaged single-particle Re ≈ 16.9 . (left) Evolution of 16 particles (from left to right and top to bottom). (right) Formation of inverted T configurations which are also observed in experiment.

3 LBE Simulation of 3D Homogeneous Isotropic Turbulence

Homogeneous isotropic turbulence in a three-dimensional periodic cubic box remains as a stand problem in the field of direct numerical simulation of turbulence. Due to the simplicity of the boundary conditions, the pseudo-spectral method can be easily used to simulate the flow. Because of its accuracy, the pseudo-spectral result is often used as a benchmark standard. Here the LBE simulation of the flow is compared with the pseudo-spectral simulation.

The parameters of the simulation are given in Table 1. The initial condition is a random velocity field with a Gaussian distribution and a compact energy spectrum. The boundary conditions are periodic in three dimensions. The Taylor microscale Reynolds number is defined as

$$\operatorname{Re}_{\lambda} = \sqrt{\frac{2K(t=0)}{3}} \frac{\lambda}{\nu} = \frac{u_{\text{RMS}}\lambda}{\nu},$$

Table 1. Parameters in lattice Boltzmann and pseudo-spectral simulations: L is the length of box side; N^3 is the system size; ν is the viscosity; u' is the RMS fluctuation of the initial velocity field; dt is the time step size; T is total integration time, Re $_{\lambda}$ is the Taylor microscale Reynolds number; and M is the Mach number.

Method	L	N^3	ν	u'	dt	T	Re_λ	М
Spectral	2π	128^{3}	0.01189	0.993311	0.002	2	35.0	0
LBE	128	128^{3}	0.009869	0.040471	1	1000	35.0	0.0687

where $K(t=0) = \langle u_0^2/2 \rangle_V = \langle 3u_{\text{RMS}}^2/2 \rangle_V$ is the volume averaged kinetic energy (of the initial zero-mean Gaussian velocity field u_0 with RMS component u_{RMS}), and λ is the transverse Taylor microscopic scale:

$$\lambda = \sqrt{15\nu u_{\rm BMS}^2/\epsilon},$$

where ϵ is the dissipation rate.

Figure 2 shows the energy spectrum E(k) as function of time, and the time evolution of the mean kinetic energy K and dissipation rate ϵ . The lattice Boltzmann results (symbols) are compared with the pseudo-spectral results (lines). The LBE results agree well with the pseudo-spectral results. Obviously the LBE method is more dissipative, especially at high wave numbers $k > \frac{1}{3}k_{\rm max}$, where $k_{\rm max} = \frac{1}{3}N$, and N is the number of mesh nodes in each direction. This is because the LBE method is only second order accurate in space and time and thus more dissipative than the pseudo-spectral method.

4 Conclusions and Discussion

The above simulations were performed on a Beowulf cluster of Pentium CPUs. For the simulation of the particulate suspension, the code consists two part: the lattice Boltzmann method for the fluid and molecular dynamics (MD) for the solid particles [17]. Even though the MD part of the code is not yet parallelized, the speed of the code still scales well with the number of CPUs up to 32 CPUs when the system size is 64^3 and with fifty particles. Presently we can easily simulate a system of a few hundred particles on our Beowulf system.

As for the simulation of the 3D homogeneous isotropic turbulence, the LBE code without optimization has the same speed as the spectral code with a Beowulf cluster of eight CPUs (about 1s per time step). However, we do expect the LBE code will scale linearly with the number of CPUs, but not the spectral code.

Our current research includes particulate suspension in fluid with high volume fraction of particles, viscoelastic and non-Newtonian fluids, and forced or free-decay homogeneous isotropic turbulence in a periodic cube by using the lattice Boltzmann method on massively parallel computers.

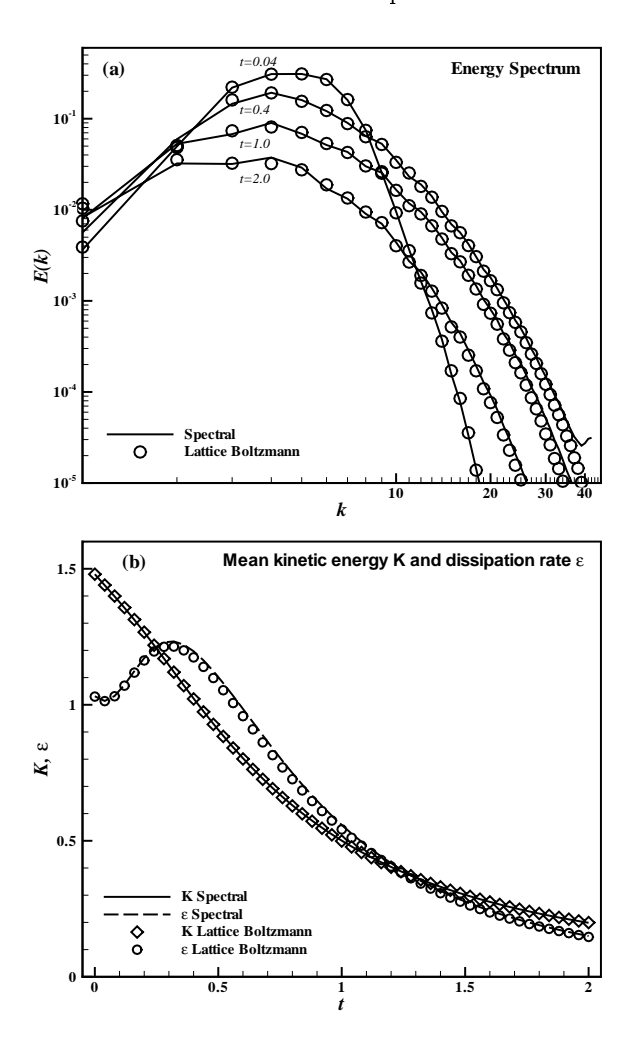


Fig. 2. LBE vs. Pseudo-spectral DNS of 3D homogeneous isotropic turbulence. System size is 128^3 . Re_{λ} = 35. (a) The energy spectrum E(k) as a function of time. (b) The decay of the mean kinetic energy K and dissipation rate ϵ . The results from the LBE simulation are scaled according to the dimensions used in the spectral simulation.

References

- 1. Bhatnagar P. L., Gross E. P., Krook M. (1954) A model for collision processes in gases. I. Small amplitude processes in charged and neutral one-component systems. Phys. Rev. **94**:511–525
- Chen H., Chen S., Matthaeus W.H. (1992) Recovery of the Navier-Stokes equations using a lattice-gas Boltzmann method. Phys. Rev. A 45:R5339-5342

- Chen S., Doolen G.D. (1998) Lattice Boltzmann method for fluid flows. Ann. Rev. Fluid Mech. 30:329–364
- Filippova O., Hänel D. (1998) Grid refinement for lattice-BGK models. J. Comput. Phys. 147:219–228
- Frisch U., Hasslacher B., Pomeau Y. (1986) Lattice-gas automata for the Navier-Stokes equation. Phys. Rev. Lett. 56:1505-1508
- Frisch U., d'Humières D., Hasslacher B., Lallemand P., Pomeau Y., Rivet J.-P. (1987) Lattice gas hydrodynamics in two and three dimensions. Complex Systems 1:649–707
- He X., Doolen G. (1997) Lattice Boltzmann method on curvilinear coordinates system: Flow around a circular cylinder. J. Comput. Phys. 134:306-315
- 8. He X., Luo L.-S. (1997) A priori derivation of the lattice Boltzmann equation. Phys. Rev. E **55**:R6333–R6336
- He X., Luo L.-S. (1997) Theory of the lattice Boltzmann equation: From the Boltzmann equation to the lattice Boltzmann equation. Phys. Rev. E 56:6811– 6817
- He X., Luo L.-S., Dembo M. (1996) Some progress in lattice Boltzmann method. Part I. Nonuniform mesh grids. J. Comput. Phys. 129:357–363
- He X., Luo L.-S., Dembo M. (1997) Some Progress in the lattice Boltzmann method. Reynolds number enhancement in simulations. Physica A 239:276–285
- Higuera F.J., Succi S., Benzi R. (1989) Lattice gas-dynamics with enhanced collisions. Europhys. Lett. 9:345–349
- Jeffery G.B. (1922) The motion of ellipsoidal particles immersed in a viscous fluid. Proc. R. London Ser. A 102:161–179
- Lallemand P., Luo L.-S. (2000) Theory of the lattice Boltzmann method: Dispersion, dissipation, isotropy, Galilean invariance, and stability. Phys. Rev. E 61:6546–6562
- 15. Luo L.-S. (2000) The lattice-gas and lattice Boltzmann methods: Past, present, and future. In: Wu J.-H., Zhu Z.-J. (Eds) Proceedings of International Conference on Applied Computational Fluid Dynamics, Beijing, China, October 17–20, 2000. Beijing, 52–83
- McNamara G. R., Zanetti G. (1988) Use of the Boltzmann equation to simulate lattice-gas automata. Phys. Rev. Lett. 61:2332–2335
- Qi D. (1999) Lattice-Boltzmann simulations of particles in non-zero-Reynoldsnumber flows. J. Fluid Mech. 385:41–62
- Qi D. (2001) Simulations of fluidization of cylindrical multiparticles in a threedimensional space. Int. J. Multiphase Flow 27:107-118
- 19. Qi D., Luo L.-S. (2001) Inertial effect of non-spherical suspension in 3D Couette flow. Submitted to Phys. Rev. Lett.
- Qian Y.H., d'Humières D., Lallemand P. (1992) Lattice BGK models for Navier-Stokes equation. Europhys. Lett. 17:479–484
- Shan X., He X. (1998) Discretization of the velocity space in the solution of the Boltzmann equation. Phys. Rev. Lett. 80:65-68
- Wolfram S. (1986) Cellular automaton fluids 1: Basic theory. J. Stat. Phys. 45:471-526